# The Spitzer Warm Mission Science Prospects

John R. Stauffer*, Vincent Mannings*, Deborah Levine*, Ranga Ram Chary*, Gillian Wilson*, Mark Lacy*, Carl Grillmair*, Sean Carey*, Susan Stolovy*, David Ciardi† and Joe Hora**

*Spitzer Science Center, Caltech 314-6, Pasadena, CA 91125, USA
†Infrared Processing and Analysis Center, Caltech 220-6, Pasadena, CA 91125, USA
**Harvard-Smithsonian Center for Astrophysics, 60 Garden St., Cambridge, MA 01238, USA

**Abstract.**
   After exhaustion of its cryogen, the Spitzer Space telescope will still have a fully functioning two-channel mid-IR camera that will have sensitivities better than any other ground or space-based telescopes until the launch of JWST. This document provides a description of the expected capabilities of Spitzer during its warm mission phase, and provides brief descriptions of several possible very large science programs that could be conducted. This information is intended to serve as input to a wide ranging discussion of the warm mission science, leading up to the Warm Mission Workshop in June 2007.

## 1. INTRODUCTION

The Spitzer Space Telescope passed a milestone of three years in orbit in August 2006, with enough cryogen for another approximately 2.5 years in its nominal mission profile. We are now starting the detailed process of considering how Spitzer will be operated in the post-cryogenic period, when the long-wavelength instruments will no longer provide useful data but the 3.6 and 4.5 $\mu$m channels of IRAC will still perform well. This document provides a brief review of Spitzer's current status and its expected performance capabilities during the post-cryo period. We then describe plausible changes in the way Spitzer will be operated in order to reflect the post-cryo capabilities and the expected decrease in ground-operations support.

   An important issue for the warm mission is the mix of observing projects undertaken. We believe it is untenable to continue both the time allocation and scheduling exactly in the manner of the cryogenic mission because this would require a staff size at the Spitzer Science Center (SSC) that is only modestly reduced from the current level. We believe that the only way to significantly reduce the SSC staffing level is for most of the observing time to be allocated to a few very large projects. We briefly outline how we believe this would work below. Given this model, it then becomes particularly important to have an early and wide-ranging discussion of the types of large projects best suited, and the mechanism by which those projects will be selected and managed. We address the first of those issues by providing outlines of four large projects as potential models for the type of science that can be done during the warm mission. We stress that

these projects are for purposes of illustration, and that they have not been selected. The details of how the large projects will be selected are still evolving, but the process will involve a mostly-external steering committee and an open workshop which they will organize, community-led white papers to develop detailed plans for specific potential large programs, and calls for proposals with peer-reviewed selection.

The range of science that could be done during the warm mission is extremely broad. The total amount of observing time for science could be of order 30,000 to 40,000 hours. If all of that time were devoted to a moderate depth survey (10 $\mu$Jy, 5$\sigma$) - i.e. about ten times deeper than WISE (*Wide-Area Infrared Survey Explorer*), of order 20 to 30% of the sky could be surveyed. Alternatively, a deep survey ($< 1$ $\mu$Jy, 5$\sigma$) intended to serve as a precursor to JWST observations could be obtained for of order 100 square degrees if that were the only project conducted during the warm mission. Obviously, anything in between those two extremes could also be conducted, including programs aimed at temporal variability or proper motions.

## 2. EXPECTED SPITZER SPACECRAFT CAPABILITIES IN THE WARM MISSION

The Spitzer Space Telescope has achieved exceptional science return and efficiency due in large part to the excellent performance of the spacecraft and cryo-telescope assembly (CTA). The spacecraft and cryostat have met or exceeded requirements, notably in the areas of pointing control and cryogenic lifetime. In the first 7 months of 2006, Spitzer spent 85.4% of the total elapsed time doing science or science instrument calibration. Based on our in-orbit experience to date, we believe that the Spitzer spacecraft hardware should perform well for many more years. There is no evidence that any of the redundant units on board have failed. The only system where there is some uncertainty is the spacecraft computer. In August 2006, Spitzer underwent an autonomous side-swap of the spacecraft computer (from Side-A to Side-B). No cause for the side-swap was identified, and the most probable explanation is a single-event upset, with the strong expectation that Side-A would operate normally if used. However, since the side-swap, we have continued operation on Side-B because that was deemed the conservative course of action.

During the nominal science mission, Spitzer operates one science instrument at a time, with instrument transitions occurring every 1-2 weeks on average. A sequence of preplanned science is uploaded weekly, and the spacecraft orients its high-gain antenna towards earth once or twice each day to downlink science data. At 2.2 Mb/s these downlink periods take 20-60 minutes depending upon the data volume. Spitzer cannot tolerate over-filling its mass memory, and sustained high data volumes necessitate downlinks twice per day for all MIPS campaigns and some fraction of IRAC operations. Spitzer is in an earth-trailing solar orbit and it recedes from earth at a rate of about 0.1 AU/year. This affects telecommunications, particularly toward the end of the nominal mission and during post-cryo operations.

Spitzer's limiting consumable for the nominal mission is the superfluid helium which cools both the instruments and the telescope (via venting from the cryostat). Current predictions for the end of the cryogenic mission place the date at which the cryogen

will be expended at March 2009 $\pm$ a month. This date is estimated from a measurement of the remaining helium mass based on the thermal response of the cryogen to heat dissipated into the cryostat. The only other consumable on Spitzer is cold $N_2$ gas for angular momentum management. Given current and expected use rates, there is enough $N_2$ on board for at least another ten years of operation.

Once the cryogen is expended the temperature of the telescope and the cryostat will rise. The telescope is expected to reach a steady-state temperature of 24-25K after 10-15 days, and is projected to remain in focus at that temperature. Neither MIPS nor IRS will be able take useful science data because of the elevated dark currents. The two shortest wavelength channels for IRAC at 3.6 and 4.5 $\mu$m, however, will be only slightly affected by the warmer telescope and cryostat, and it is predicted that they will operate with essentially the same sensitivity as they have for the cryogenic portion of the mission. Those two channels are the most sensitive IRAC channels now, and will remain the most sensitive cameras at those wavelengths until JWST is launched.

The spacecraft itself is basically unaffected by the depletion of the cryogen. Operations will continue with only minimal changes from the nominal operations scenario. Most of the small number of changes that are planned will help facilitate operating the mission with the reduced ground resources expected to be available during the post-cryogen phase. We expect to operate typically with just one downlink per day, and possibly with two-week-long sequences rather than one-week long sequences. For a constant data volume, the single downlink per day would become longer as the distance from earth increases and the downlink rate decreases. However, compared to now, the data volume will be effectively halved because only two of IRAC's four channels will be operating. The two factors approximately cancel each other. If both transmitters aboard the spacecraft are used, it can support a downlink rate of half the nominal rate, or 1.1 Mb/s out to the end of post-cryogenic operations. With a single transmitter as in nominal operations, the final data rate would be about half that. The maximum length of a downlink is 2.5 hours. While not a certainty, it is entirely possible that downlink data volume will not limit the observing cadence with Spitzer during the post-cryogen period any differently than has been true during the cryogenic mission.

Spitzer's operational pointing zone (OPZ) is limited by the sun-Spitzer geometry, and that does not change over the course of the mission. However, in order to downlink data to Earth, the spacecraft must be able to orient its fixed high gain antenna to point towards the Earth. The high-gain antenna is located on the bottom of the spacecraft and points approximately opposite to the telescope boresight direction. As Spitzer drifts away from the Earth, the orientation it has to assume in order to downlink data gradually causes the telescope pointing direction to approach the edge of the OPZ. Toward the end of the warm mission, the nominal geometry begins to place the downlink orientation outside the OPZ. This can be tolerated initially by pointing the high-gain antenna slightly away from the nominal direction, reducing bandwidth in exchange for lengthening the duration of the mission. As another telecommunications constraint, should Spitzer enter safe mode, the signal from its low-gain antennae when it is rotating about the sun-line must be receivable at earth, and the spacecraft must be able to receive uplink signal from earth in order to recover from safing. Given our current best estimates, it is this latter limitation that we will run up against first and that will signal the end of the post-cryo mission.

Based on current estimates, the end of the post-cryo phase will occur in January 2014. To operate past early November 2013, the OPZ will need to be extended by about 5 degrees to permit downlink orientation, but analysis demonstrates this will be acceptable. At or near the end of 2013, the angle between the low-gain antennas and earth in safe mode exceeds 40 degrees, and the uplink bit rate would drop below the minimum allowed - and this is not mitigable.

More details about the design and operation of Spitzer and the characteristics of the IRAC camera can be found at the Spitzer website[1]. A detailed description of the IRAC camera design and performance can be found in Fazio *et al.* [1].

# 3. EXPECTED CAPABILITIES OF IRAC IN THE WARM MISSION ERA

## 3.1. Summary

During the warm mission the IRAC 3.6 and 4.5 $\mu$m channels will operate near a temperature of 30K, and will experience little or no degradation compared to their nominal mission performance. Based on thermal and optical models of the telescope and IRAC, a focus adjustment using the telescope secondary mirror mechanism is not expected to be required to maintain the nominal mission optical performance.

## 3.2. Telescope and IRAC Optics

According to a thermal analysis of the observatory, after the cryogens are exhausted the telescope and multiple instrument chamber (MIC) are expected to warm up over a period of about 10 days, and reach an equilibrium temperature of $25 - 29$K. This range is for a nominal IRAC focal plane power dissipation.

The Spitzer telescope does have the ability to adjust its focus by moving the secondary mirror assembly. The IRAC camera itself does not include a focus mechanism. During the initial in-orbit checkout period in 2003, the secondary mirror assembly was moved twice in order to achieve a location which produced acceptably focused images for all three instruments. The telescope focus was monitored during the cooldown after launch, and no significant change in focus position was detected below 55K. The difference between the case of cooldown after launch and the post-cryo mission is that the MIC and inner cryostat were at 1.2K during the initial cooldown, whereas after the cryogens are expended the MIC and cryostat will warm up with the telescope and stabilize at $\sim$25K. However, this is not expected to cause a significant focus shift. In the IRAC instrument, the lens materials will experience a small change in the index of refraction which will cause a small shift in the instrument focus and point response function (PRF), but analysis performed by the IRAC team indicates that this should not significantly affect

---

[1] see http://ssc.spitzer.caltech.edu

the instrument performance. Therefore, the intention is to obtain image characterization measurements at the new temperature equilibrium point (i.e. 10+ days after cryogen exhaustion), but a refocus of the telescope should not be required. As a precaution, however, the project recently completed a planning exercise to make sure all of the tools and expertise would be available to refocus Spitzer during the post-cryo check-out phase if that were necessary. The conclusion of that exercise was that the team was ready for this eventuality, and that it should not consume a significant amount of telescope time.

## 3.3. Detector Performance

It was known from pre-launch testing of the InSb detectors used for the 3.6 and 4.5 $\mu$m channels that the dark current in the arrays was sufficiently low to allow for their use in a post-cryo mission. In order to better characterize their performance near 30K, a series of tests were performed recently at the University of Rochester by McMurtry, Pipher, and Forrest [2]. The characteristics of these devices are considered to closely match the in-flight devices.

The results showed that operation at 30K did not significantly degrade the detector performance. The dark current is not significantly higher; it is expected to remain below 1 electron/sec until about 37K, so there is ample margin. The quantum efficiency of the devices should be unchanged. The read noise will likely be the same or slightly higher. However, in long exposures where the zodiacal background will dominate the noise, it will not affect the instrument sensitivity. The level of residual images caused by saturating sources is seen to increase, but they also decay faster so on balance are not significantly worse. The current IRAC pipeline contains flags for marking residual image-affected pixels and excluding them from mosaics made with IRAC images. No significant new types of image artifacts or instabilities were observed during the 30K tests over what is currently seen in the IRAC nominal mission data.

We have also monitored the number of noisy, hot, dead, and otherwise scientifically unusable pixels in the IRAC detectors during the nominal mission up through the end of 2005. This period has included two extremely intense solar flares in November 2003 and January 2005. In the 3.6 and 4.5 $\mu$m channels, no increase in the number of noisy, hot or dead pixels was noted. Therefore we would expect no significant increase in their number during the warm mission - even considering the fact that the next solar maximum should occur around 2011 (in the middle of the warm mission).

## 4. SPITZER/IRAC COMPARED TO OTHER FACILITIES

The Spitzer warm mission will be conducted in an environment where it is expected that COROT will have been launched a few years earlier, Kepler will have just been launched, WISE will be launched during the same year, and where JWST would be expecting launch within about four years. The Spitzer warm mission should be planned to complement what can be done with WISE and to help prepare scientists to utilize JWST as efficiently as possible.

**TABLE 1.**  Sensitivity And Areal Coverage For Different AOR Types

| AOR Type | Number Dithers | Frame Time(sec) | Ch1 (5$\sigma$,$\mu$Jy) | Ch2 (5$\sigma$,$\mu$Jy) | Area in 1000 hr Sq.Deg. | Example |
|---|---|---|---|---|---|---|
| Shallow | 3 | 2 | 100. | 110. | 400 | GLIMPSE,WISE |
| Wide | 4 | 12 | 8.5 | 12.5 | 225 | 360GLIMPSE |
| Moderate | 4 | 30 | 3.5 | 6. | 125 | z>1 clusters |
| Deep | 6 | 100 | 1.3 | 2.5 | 25 | |
| Very Deep | 900 | 100 | 0.1 | 0.2 | 0.25 | High-z |

WISE is designed to provide a map of the complete sky in four passbands (3.3, 4.7, 12 and 24 microns). Therefore, its two short wavelength bands approximately duplicate the two IRAC bands available for use in the warm mission. However, because WISE has a smaller primary mirror and is designed to obtain a shallow survey of the entire sky, it has a comparatively low sensitivity - the required 5$\sigma$ sensitivity levels are 120 and 160 $\mu$Jy, respectively, at 3.3 and 4.7 microns. The lower angular resolution for WISE (PSF about 2.5 times broader than for IRAC) means that WISE will have more difficulty in crowded fields than IRAC (e.g. the galactic plane or star clusters).

By contrast, JWST's NIRCAM is **very** sensitive and has a very good angular resolution, but is not well-suited to covering large areas of the sky. NIRCAM will have a large number of broad-band filters covering the 1-5 micron wavelength region and a PSF size of order 0.1 arcseconds in the 3 to 5 micron wavelength range. The five sigma sensitivities for a 1000 second exposure (the nominal exposure time expected for NIRCAM) are of order 10 and 20 nJy for the broad-band filters near 3.5 and 4.6 microns. JWST's observing capabilities are still being determined, but it is expected that a combination of data volume issues, commanding issues and slew/acquire times will significantly limit the ability to image large areal regions. A current estimate is that an area of approximately 0.5 square degree could be imaged in a 24 hour period down to a 5$\sigma$ point-source sensitivity of about 100 nJy at 4.6 microns using an integration time of around 50 seconds per field (shorter integration times would not appreciably increase the survey area because most of the clock time is consumed in overheads and slew/settle). The depth would be comparable to the Spitzer GOODS program. One of the most valuable contributions for the Spitzer warm mission may be to provide deep enough surveys of relatively wide regions to provide the first targets for JWST once JWST is in orbit. That is, obviating a need for JWST to use its precious observing time for wide-shallow surveys of its own in order to provide target lists for followup deeper imaging or spectroscopy.

Figure 1 provides a graphical comparison of the combination of sensitivity and areal coverage for WISE, JWST/NIRCAM and Spitzer/IRAC. The figure illustrates that the niche for Spitzer/IRAC is for surveying to depths not reachable with WISE and for areal coverage which would be prohibitively expensive in time for JWST. Table 1 provides sensitivity levels for several different integration times for IRAC Ch1 (3.6$\mu$m) and Ch2 (4.5$\mu$m), with links to the possible large projects which we describe later.

As one example, consider the case of a program to survey for clusters of galaxies with $1 < z < 2$ (see section 6.1). In order to identify enough new clusters to significantly
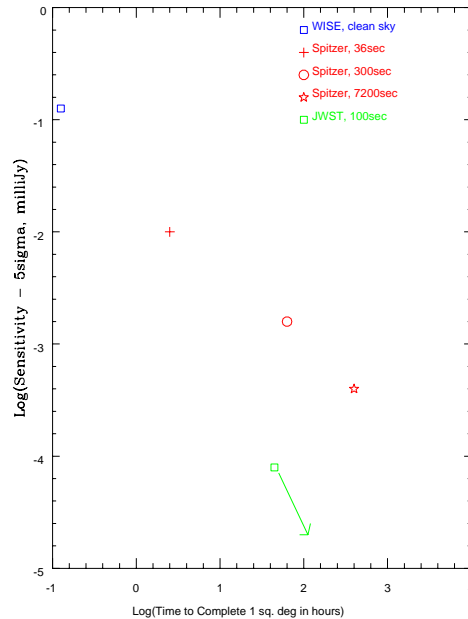
**FIGURE 1.** Comparison of the time needed to conduct imaging surveys of a given area of the sky for WISE, Spitzer/IRAC and JWST/NIRCAM. For Spitzer, the three symbols correspond to surveys with total integration times per point on the sky of 36, 300 and 7200 seconds.

advance this field, the area surveyed needs to be of order 200 square degrees, or more. In order to identify these clusters requires being able to detect cluster members down to two and a half times fainter than an L∗ galaxy, corresponding to about 4 $\mu$Jy, five sigma at 3.6 $\mu$m. These clusters will therefore be completely undetected in the WISE all-sky survey. To complete the required sky coverage with JWST, however, would take of order a year of dedicated observing. Spitzer/IRAC could complete the survey in three to four months, and do so in time to complete full analysis of the data and to propose follow-up detailed NIRCam imaging once JWST is launched.

As another example, consider a project to confirm candidate Y dwarfs identified with WISE. If WISE only completes one epoch of observations for the full sky before it exhausts its cryogen, only a few of the nearest Y dwarfs will be detected in two or more bands - most will be one-channel detections (the 4.5 $\mu$m band). It is expected there will be tens of thousands of such 4.5 $\mu$m-only sources, the great majority of which will be spurious. Obtaining good S/N IRAC 3.6 $\mu$m and 4.5 $\mu$m photometry for these sources would be sufficient to confirm or reject these sources as Y dwarfs, and would take only of order 1 minute of observing time each. A couple dozen such sources could be observed each day with IRAC in a snapshot mode with relatively little impact on the primary program(s) conducted that day, and hence thousands could be covered each year. Attempting to do the same thing with JWST/NIRCAM would require much more telescope time due to the much slower slew/settle times for JWST, and so would not be feasible. A similar program with ground-based facilities would also be prohibitive in terms of number of nights on big telescopes.
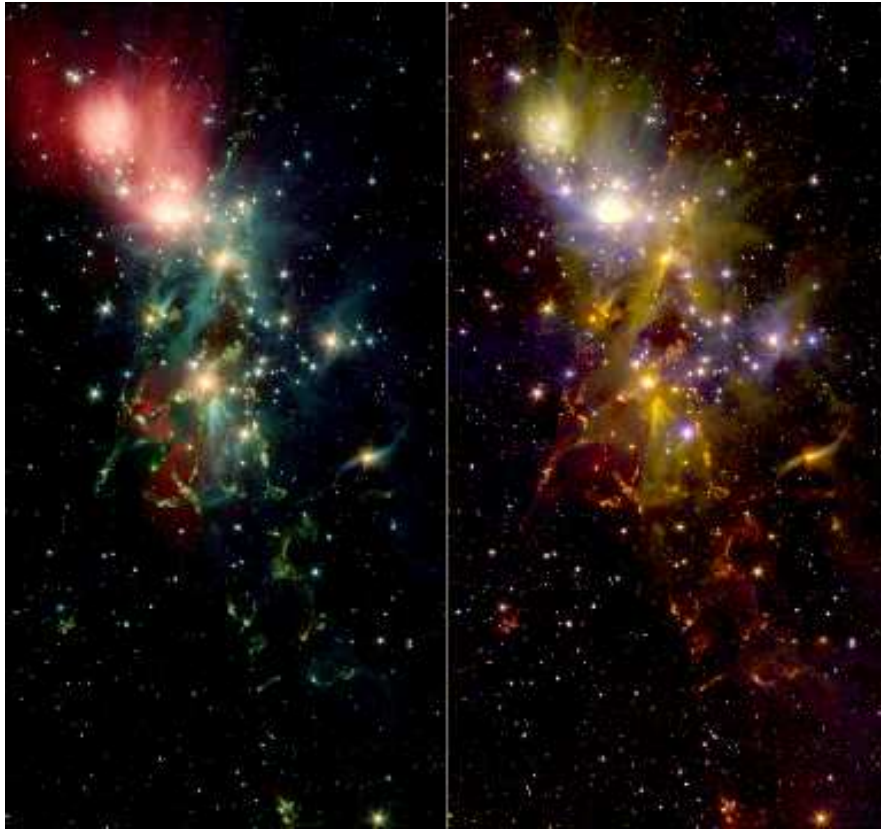
**FIGURE 2.** (a) Three-color (IRAC 3.6, 4.5 and 5.8 $\mu$m) image of the NGC1333 star-forming region (NASA/JPL-Caltech/R.A. Gutermuth). (b) The same region, but using 2MASS K-band as the blue filter, and IRAC 3.6 and 4.5 $\mu$m as the green and red filters.

For some types of science, it is useful to have data in more than two bandpasses. A pertinent example is the search for young stars with primordial, circumstellar disks in star-forming regions. Such searches are well-suited to the cryogenic IRAC because a two-color diagram (Ch1 minus Ch2 vs. Ch3 minus Ch4) clearly separates pure photospheres, from classical T Tauri stars with disks and from even younger stars with infalling envelopes. In the warm mission, an IRAC-only survey with just channel 1 and 2 would not be able to discriminate stars that are simply heavily reddened from those with disks or envelopes. Much of this science could be recovered, however, by combining the IRAC imaging with a ground-based survey in the near-IR (J, H or K). From a purely aesthetic viewpoint, Figure 2 illustrates that the latter type of survey can produce 3-color images with as much visual impact as the current IRAC-only images.

## 5. OPERATIONAL PLANS DURING THE WARM MISSION

The current staffing level for the SSC is sufficient to support the nominal mission − but just barely. Once the cryogen runs out, support of new Spitzer observations will no longer require staffing for the two retired instruments (MIPS and IRS). However, this

represents a small fraction of the anticipated steady-state staffing level required for the SSC during the warm mission period. A significant fraction of the work for the Science User Support team (SUST) is directly proportional to the number of approved programs, with a premium for programs led by inexperienced Spitzer users. By mandating that all but a small fraction of the observing time be devoted to very large projects, the workload, and hence the staffing level, for the SUST should be significantly reduced. The Operations Planning and Scheduling Team (OPST) workload would also decrease with fewer projects (fewer special cases, less interaction with observers), and the workload of the Community Affairs team could decrease significantly if the yearly TAC meeting could be simplified and if the number of proposals submitted, reviewed and approved could be reduced appreciably.

It is expected that the IRAC AOT will not undergo significant changes for the warm mission (other than to reflect the fact that only two arrays will be used). Because there will no longer be transitions between instruments, it should be possible to reduce the number and frequency of calibration observations, thus providing even more observing time for science. It is probable that we will try to minimize the number of observations scheduled for targets-of-opportunity . In order to make the most of the large programs, we will likely require the teams proposing those programs to produce enhanced data products (in particular, source lists and photometry) or we will solicit archival proposals to perform that function.

It is possible that one or more large projects may be identified which are most efficiently implemented by the SSC as a service to the community. In that case, the data from the program would be made public without any proprietary period and special effort would be made to fund archival proposals to mine the data from that program; enhanced or higher-level data products could also be generated by the SSC or by proposing teams.

## 6.  EXAMPLES OF LARGE "LEGACY" PROJECTS FOR THE WARM MISSION

As a means to begin the conversation about the science programs that should be pursued during the Spitzer warm mission, we provide below a few illustrative, large programs. These are *not* meant to pre-empt other ideas or to establish precedence for any particular teams. They are simply explorations of ideas for large and scientifically exciting projects that would have significant impact. The programs that will in fact be conducted will be chosen via an open selection process whose nature will be defined with community input during the upcoming year.

### 6.1.  The Case for a Wide, Moderate Depth Extragalactic Survey

The tremendous power of deep multipassband datasets has become increasingly apparent over the last few years. Multipurpose surveys (e.g., GOODS, COSMOS, AEGIS) have very successfully synergised datasets to study galaxy formation and evolution to high redshift. However, the fields studied have been very small, $\sim 1$ deg$^2$ and are there-

fore subject to cosmic variance. Moreover, the fields are of limited use for studying the most clustered and/or rare sources e.g., extremely red objects (EROs), ULIRGs, and superclusters. Larger area surveys are clearly necessary.

The SWIRE Legacy Survey[2], was the largest of the original six Spitzer Legacy Programs. SWIRE's six wide-area, high galactic latitude fields were imaged by Spitzer at 3.6, 4.5, 5.7, 8.0, 24, 70 and $160\mu$m over a total of $\sim 50$ deg$^2$. The SWIRE dataset has been used to trace the evolution of dusty, star-forming galaxies, evolved stellar populations, and active galactic nuclei as a function of environment (Lonsdale *et al.* [3, 4], Oliver *et al.* [5], Babbedge *et al.* [6], Rowan-Robinson *et al.* [7], Farrah *et al.* [8]). However, even SWIRE is not sufficiently large to discover more than a handful of the most massive clusters at $z > 1.5$.

Astro-F and WISE will perform shallow all-sky IR surveys and JWST will perform very deep pencil beam surveys. This leaves an obvious unfilled niche - deep multipass-band surveys on scales of hundreds of square degrees. Note that the IR imaging component of such a deep wide-field survey can only be performed from space. An IRAC SWIRE-depth survey of 200-300 square degrees would take $2000 - 3000$ hours (i.e., three to four months) to perform. CFHT's WIRCAM, the largest existing ground-based IR camera, would require $\sim 2000$ **nights** to reach the same depth at K for an equivalent survey, and would produce more variable photometry across the fields than can be achieved with the ultrastable IRAC camera.

MegaCam on the CFHT is in the process of filling this large-area niche at optical passbands, observing what will be the foremost multi-passband optical dataset for many years to come, the $u^{\star}g'r'i'z'$ CFHT 170 deg$^2$ "Wide" Legacy Survey[3]. This area is much too large for redshifts to be determined spectroscopically, one must rely on photometric redshift estimation techniques. However, accurate estimation of photometric redshifts at $z > 1$ is impossible with an optical dataset alone (Ilbert [9]). And yet, frustratingly, the redshift range $1 < z < 2$ is exactly the redshift regime one would like to study. It is of particular importance for three reasons, a) It is the redshift at which dark energy begins to dominate over dark matter. b) It corresponds to the "redshift desert" where prominent spectral features are notoriously difficult to measure in the optical: more is known about galaxy evolution at $z > 2$ (from e.g. Lyman-break studies) than at $1 < z < 2$ c) It is the epoch of mass assembly in galaxies.

The CFHTLS fields (and indeed, those proposed by several future large ground-based optical surveys e.g., PanSTARRS, LSST), would be well-matched to an IRAC imaging survey. The CFHTLS optical survey should be complete by 2008, a year or more prior to the beginning of the Spitzer warm mission. The addition of IRAC passbands would facilitate reliable photometric redshifts to $z \sim 2$ [the redshift regime where the 4.5 and/or $3.6\mu$m channel unequivocally sample longward of the 1.6 $\mu$m bump feature, found in all "normal" galaxies (Sawicki [10])]. The resulting combined optical-infrared survey, would be a one-of-a-kind dataset, opening up the $1 < z < 2$ universe, and enabling a variety of galaxy evolution and cosmological applications. This dataset would be impossible to surpass for at least another decade.

---

**Clusters Of Galaxies at** $1 < z < 2$ **As Dark Energy Constraints:** Galaxy clusters form at the highest peaks in the primordial density field, and as a result, their abundance and spatial distribution are very sensitive to the underlying cosmology. Clusters at $z < 1$ are now proving themselves useful tools for constraining cosmological parameters, especially with respect to the matter density, $\Omega_m$, and the amplitude of the matter power spectrum, $\sigma_8$ (Gladders et al 2006). A sample of clusters in the redshift range $z < 1 < 2$, however, would provide strongest constraints on the nature of the dark energy, arguably the most important problem in cosmology today.

**Combining Cosmological Constraints:** The improved accuracy which IRAC would bring to the estimation of photometric redshifts would translate into improvements in the constraints achievable from any weak lensing cosmic shear analysis (Refregier [12], Schneider [13], Hoekstra [14]). One would ultimately wish to combine the constraints from the cluster and lensing surveys with those available from Baryon Acoustic Oscillations[4] and Type Ia Supernovae, and of course from the Cosmic Microwave Background.

**Stellar Mass Density Evolution:** Mid-IR observations are ideally suited to tracing the accumulation of stellar mass in galaxies (Labbé *et al.* [15], Shapley *et al.* [16], Rigopoulou [17]). Note that at $z > 0.4$, even a $K$-band selected dataset can only sample shortward of restframe $1.6\mu$m, and so stellar mass estimates for galaxies above $z = 0.4$ are subject to increasing uncertainties, especially w.r.t. dust content. A wide-field seven-passband dataset would allow an unprecedented measurement of the build-up of stellar mass in galaxies from $z = 2$. Galaxies could be classified by luminosity, morphological type (early or late) and environment (field or cluster), and the epoch of mass assembly determined for each type.

**The Relationship Between Stellar Mass And Total Mass:** A main science driver behind the CFHTLS Wide Survey (and future surveys such as PanSTARRS and LSST) is the application of of various weak gravitational lensing techniques e.g., the CFHTLS Wide Survey will measure galaxy dark matter halo evolution to $z \sim 1$, but will still be limited to measuring galaxy luminosities in the restframe optical. The IRAC observations will complement the weak lensing analysis in two important ways. Firstly, IRAC imaging will greatly improve photometric redshifts estimates of the source (and lens) galaxies (most of the source galaxies will lie at $1 < z < 2$). This is vital to break the degeneracy which exists between the source redshift distribution $N(z)$ and the mass normalization. Secondly, since the IRAC observations will allow stellar mass estimates of the lens galaxy population, and these can be subdivided by redshift, luminosity and spectral type, this dataset will provide a measurement of the evolution of baryons relative to the dark matter out to at least $z = 1$. These data will therefore allow a direct test of assumptions relating the physics of feedback e.g., cooling flow suppression by AGN in massive galaxies (Croton *et al.* [18]) to the evolution of the dark matter halos.

On larger scales, the dark matter distribution can be mapped using standard mass reconstruction techniques. The ability to reliably group source galaxies by redshift, allows one to perform "mass tomography". By careful selection of the source galaxy

---

[4] We might also be able to make the case for the dataset discussed here for the warm mission as being of use as a BAO probe or pathfinder survey.

redshift distribution, one can tune the redshift range of the (intervening) dark matter of interest. By selecting several source galaxy redshift distributions in turn, one can create 3D maps of the mass distribution. These mass maps could then be compared to the distribution of galaxies as a function of redshift, luminosity and morphological type, revealing the evolution of baryons versus dark matter on large scales.

**Galaxy Clustering Evolution:** It will also be possible to measure galaxy clustering as a function of redshift, luminosity, scale, and morphological type. These measurements would provide constraints on theories of galaxy formation and evolution.

**Obscured AGN:** Although the most highly-obscured AGN require longer wavelengths to be identified, there is a significant population of moderately-reddened quasars which can be found even at near-infrared wavelengths (Cutri *et al.* [19], Glikman *et al.* [20]). An IRAC survey based either on photometric techniques for identification of quasars in the infrared (Warren *et al.* [21]) or on matching to radio surveys such as FIRST or upcoming surveys with LOFAR would enable us to find several thousand moderately-obscured quasars. With a sample of this size to compare with the existing SDSS sample of normal quasars (whose flux limit is well-matched to the IRAC surveys), we can search for evidence of an evolutionary link between dusty and normal quasars through studies of their host galaxies (Sanders *et al.* [22]) and test models for the dependence of the fraction of dusty quasars on the luminosity of the AGN (Lawrence [23]).

## 6.2. A Deep Survey for High-z Galaxies and Supernovae

### 6.2.1. Galaxies From $0.5 < z < 7$: Clustering and Evolution

Spitzer IRAC observations in the $3.6\mu$m and $4.5\mu$m passband, by virtue of tracing redshifted optical/near-infrared light, provide an excellent measurement of the stellar mass in galaxies out to $z \sim 6$. Spitzer observations conducted as part of the Great Observatories Origins Deep Survey (Dickinson *et al.* [24]) have revealed that many galaxies build up stellar masses comparable to that of the Milky Way within 1 Gyr of the Big Bang (Chary *et al.* [25], Yan *et al.* [26], Eyles *et al.* [27]). Although massive by themselves, the stellar mass in these galaxies is only a fraction ($\ll 1\%$) of the total co-moving matter density which is dominated by dark matter. This dark matter primarily resides in the halos of galaxies and within $10^{13-14}$ $M_\odot$ structures and superstructures. Detecting the former requires observing the spatially resolved dynamics of stars within galaxies which is nearly impossible in the distant Universe. The formation and evolution of clusters and superclusters on the other hand can be traced by simply measuring the redshift evolution in the clustering properties of galaxies on angular size scales of 3-10 Mpc. Comparison of the redshift evolution of galaxy clustering with those estimated from simulations of the large scale structure such as the Millennium simulation (Springel *et al.* [28]) can then be used to test the "hierarchical structure formation in standard cold dark matter" paradigm (Figure 3). This paradigm is under threat due to the tentative evidence from the dynamics of nearby dwarf spheroidal galaxies which indicates the presence of "warm" dark matter in the cores of these galaxies (Wilkinson *et al.* [29]). The effect of such "warm" dark matter would be to weaken the clustering signal on short

**TABLE 2.** Deep Survey Fields

| Field | Area | Coordinates | No. of Redshifts | Current IRAC coverage |
|-------|------|-------------|------------------|------------------------|
| GOODS-N | $30' \times 30'$ | 12h36m, +62d14m | $\sim$3000 | 25 hr Central 165 arcmin$^2$ |
| GOODS-S | $30' \times 30'$ | 03h32m, -27d48m | $\sim$2200 | 3 hr depth entire field |
| | | | | 25 hr Central 165 arcmin$^2$ |
| EGS | $10' \times 90'$ | 14h19m, +52d43m | $\sim$12000 | 3 hr depth entire field |

co-moving distances in the distant Universe and enhance the clustering signal on large angular scales

Accurately measuring the evolution of the clustering amplitude of galaxies as a function of redshift requires the detection of $\sim$1000s of typical $\gtrsim 10^9$ M$_\odot$ galaxies out to $z \sim 6$. This can be achieved by observing fields which have the best spectroscopic redshift surveys and the best multiwavelength imaging data which also enable accurate photometric redshifts to be determined. There are three fields (Table 1) which match these requirements - the GOODS-N field, the GOODS-S field and the Extended Groth Strip (EGS). These fields encompass an area of 900 arcmin$^2$ each resulting in a total areal coverage of 2700 arcmin$^2$ which is $1.5\times$ the solid angle subtended by the full moon.

The 400 arcmin$^2$ of deep Hubble/ACS observations in the GOODS fields have yielded $\sim$500 candidate objects at $z \sim 6$ (Bouwens *et al.* [30]). Of these, only about 12% have been spectroscopically confirmed. The 2700 arcmin$^2$ area would therefore yield more than 3000 candidate objects at $z \sim 6$ which could be spectroscopically followed up by JWST.

### 6.2.2. Supernovae From the First Stars at $z > 6$

Wilkinson Microwave Anisotropy Probe results indicate that the process of reionization started early, maybe around $z \sim 10$. The star-formation histories of $z > 5$ field galaxies are insufficient to account for the reionizing flux unless the duration of the starburst is extremely short, lasting less than 6% of the time (Chary *et al.* [25]). An alternative to the short starburst timescale is that the stellar mass function is biased towards high masses which would result in a greater flux of ionizing photons for each unit of baryon that goes into stars. Since star-formation at high redshift likely takes place in low metallicity environments, the optical depth of the star to its own flux is low. Unlike at low redshift, where massive stars blow themselves apart from their radiation pressure, the absence of metals at high redshift results in the star being stable till the fuel is exhausted (Heger *et al.* [31]). Such massive stars, referred to as Population III stars, are thought to end up as pair-creation supernovae whose light curve and spectrum are uncertain (Scannapieco *et al.* [32]). At redshifts of 10 and beyond, the light from these supernovae is time-dilated and can only be detected as near-infrared sources that are variable over timescales of months. One of the biggest problems in searching for such distant supernovae in the GOODS field has been the limited area covered in two epochs separated by a few months. Only 1/3 of the GOODS area, i.e. $\sim$100 arcmin$^2$ are sensi-

tive to objects that are variable over long timescales. Even in this limited area, due to the rotation of the asymmetric Spitzer point spread function with time, the identification of variable sources is limited to isolated sources which are at relatively bright flux densities. The model light curves of pair-creation supernovae from >100 M$_\odot$ stars at $z \sim 10 - 20$, although uncertain, are thought to be at the detection limit of 25 hrs of Spitzer observations at 3.6$\mu$m and 4.5$\mu$m (Figure 4).

By observing the 2700 arcmin$^2$ area of the three fields in Table 1 for 25 hrs - separated as two epochs of 12.5 hrs depth, it would be possible to observe the same patch of sky with the same position angle. This will minimize residuals due to the PSF rotation and allow better pairwise subtraction of data taken at different epochs enabling the sensitivity to variable sources to be pushed down the background limited values rather than the confusion limited value. Even non-detections at these faint flux limits will place strong constraints on the spectrum and energetics of these exotic objects and assess if they are sufficient to account for reionization. Such a uniform, "wide" area survey will also enable an accurate measurement of the fluctuations in the extragalactic background light. The measurement of these fluctuations in a deep Spitzer IRAC observation have placed the first constraints on the existence of high redshift Population III stars (Kashlinksy *et al.* [33]).

To reiterate, the deep survey would be comprised of imaging for the total 2700 arcmin$^2$ region of the three fields in Table 1 to the GOODS depth of 25 hours in the 3.6$\mu$m and 4.5$\mu$m passbands. Including overheads, we estimate this would take about ~3600 hrs of observing time. The areal extent of these fields is determined by the quality of the Hubble/ACS optical imaging data, the Chandra X-ray data, the existing Spitzer MIPS far-infrared imaging data and the VLA/radio, Keck and ESO/VLT spectroscopic data. By ensuring a perfect areal overlap between the deepest surveys performed by NASA's 3 Great Observatories and the wealth of multiwavelength data from the largest ground-based telescopes, this would provide a lasting legacy in the study of galaxy evolution, structure formation and first generation of stars in time for follow-up with future facilities like the James Webb Space Telescope.

### 6.3. A 360 Degree GLIMPSE of the Galactic Plane

Mid-infrared, large scale, shallow surveys of the Galactic plane and other regions of our Galaxy have already provided a wealth of data on Galactic structure, the physics of star formation and the evolution of the Milky Way. The GLIMPSE project (Benjamin *et al.* [34]) used IRAC to survey the inner Galactic plane from $-65 < l < 65$ and $|b| < 1$ (in combination with the Galactic center observations of Stolovy [35]). GLIMPSE has revealed new star clusters hidden by the extinction of the Galactic plane (Mercer *et al.* [36]), numerous previously uncataloged star forming regions (Mercer *et al.* [37]) and furthered our understanding of Galactic structure (Benjamin *et al.* [38]).

The proposed project is to finish the Spitzer mid-IR census of the Galactic plane by mapping the extent of the thick disk around the midplane of the Galaxy over the entire longitude range. The observations will trace the warp of the Galactic disk in the outer Galaxy. The survey would address three main science topics: the extent of star formation
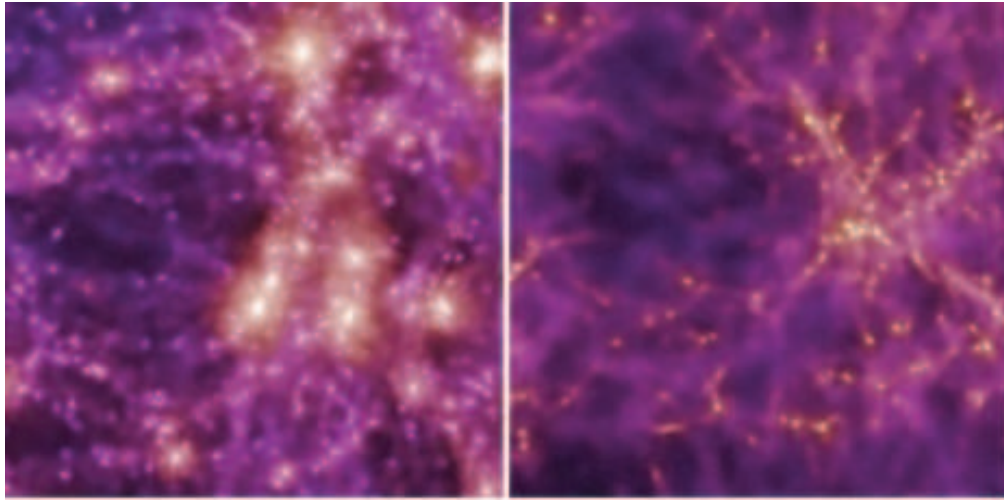
**FIGURE 3.** Evolution in the dark matter distribution in a 30 arcmin x 30 arcmin between $z \sim 1$ (left) and $z \sim 5$ (right) from the Millennium simulations (reprinted from Springel *et al.* [28]). Clearly, the dark matter and therefore, the galaxies are much more strongly clustered at $z \sim 1$ than at $z \sim 5$. By tracing the evolution of clustering of galaxies in redshift bins and comparing them to simulations of structure formation in dark matter dominated models, we can constrain the nature of dark matter. In "warm" dark matter scenarios, the clustering of galaxies will have more power on larger angular scales and less power on small scales. A survey of the type proposed would be able to measure the clustering amplitude of galaxies on scales up to $10h^{-1}$ Mpc while the current GOODS observations are limited to correlation lengths of $\sim 3h^{-1}$ Mpc.
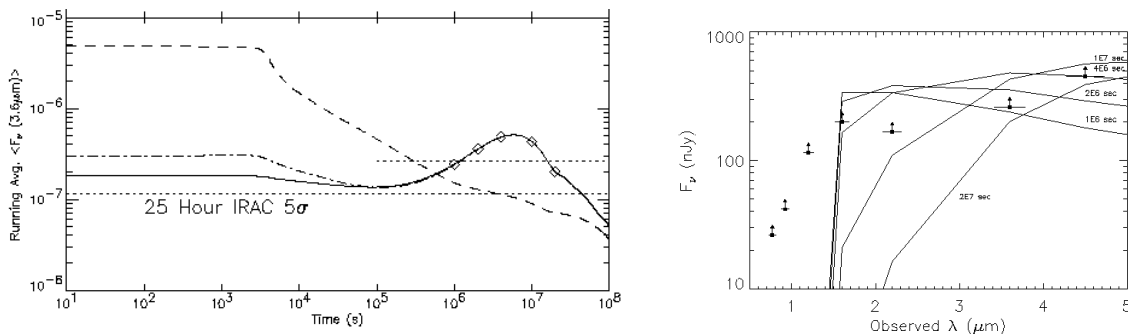


**FIGURE 4.** Plot showing the characteristics of a pair creation supernova from a 200 $M_\odot$ star exploding at redshift of 10. The left hand panel shows the light curve in the $3.6\mu$m channel (solid line). The right hand panel shows the time evolution of the spectral energy distribution of such a supernova. Also shown in the right hand panel are the sensitivity limits of the GOODS Hubble and Spitzer observations as well as the ESO/VLT near-infrared imaging data. The ability to constrain the presence of these objects is currently hindered by the 100 arcmin$^2$ area in GOODS which has two epoch coverage and the rotation of the Spitzer point spread function over these two epochs. If present, these variable sources might be remnants of the first generation of stars forming in the Universe.

in the outer Galactic disk, the number of evolved stars (particularly massive evolved stars) in the Galactic disk, and the structure of the Galaxy along heavily extincted lines of sight.

*Far-outer Galaxy star formation.* Ongoing star formation at Galactocentric distances up to 19 kpc has recently been identified (Kobayashi *et al.* [39]). The lower metallicity, low volume density of molecular clouds and longer time between spiral arm passages in the outer Galaxy provides a very different environment for star formation than inside the Solar circle. The role of environmental factors and triggering on star formation efficiency can be examined by comparing star formation as a function of Galactocentric radius. A uniform census of star formation at the periphery of our Galaxy can be used to understand the distribution of star formation at the edges of other spiral galaxies.

In addition to being sensitive to the point source emission from protostars, the 3.6 $\mu$m band is sensitive to the diffuse dust emission from PAHs excited by young stars. Molecular outflows associated with class 0 and class I protostars can be detected by an enhancement in the 4.5 $\mu$m band which contains the $H_2$ $v$=0-0 S(9) line. Molecular outflows of modest extent (0.1 pc) can be resolved at a distance of up to 10 kpc by IRAC. Figure 5 displays a young star forming cluster towards l $\sim$ 180 degrees (NGC 1893; distance of $\sim$ 6 kpc) at K band, 3.6 and 4.5$\mu$m. The image is representative of the quality of the proposed IRAC observations and demonstrates how the mid-IR bands reveal embedded star formation and that interesting star-forming regions exist well outside the longitude range covered by the existing GLIMPSE surveys.

*Evolved stellar populations.* The number of identified, evolved massive stars in the Galaxy is an order of magnitude smaller than predicted from observations of other spiral galaxies (Shara *et al.* [40]). The proposed survey will be able to identify all Wolf-Rayet stars in the surveyed field throughout the extent of the Galactic disk. Previously unknown AGB stars will be detected in abundance. The role of these stars on replenishing metals in the ISM and their effect on the Galactocentric metallicity gradient can be examined with this unbiased survey.

*Galactic structure along extincted lines of sight.* Near-infrared investigations have recently been able to map well the distribution of stars in the thick disk of the Galaxy (Cabera-Lavers *et al.* [41]). However, there is substantial extinction in the Galactic plane even at K-band (Marshall *et al.* [42]) particularly along lines of sight containing massive star forming regions such as Cygnus X and spiral arm tangent points. Recent work by Frieswijk *et al.* [43] has shown that near-infrared extinction is also important along lines of sight in the 2nd and 3rd quadrants. The IRAC bands are much less affected by extinction ($A_K \sim 5 \times A_{4.5}$; Weingartner and Draine [44]) and can probe the distribution of stars more effectively along high extinction lines of sight.

*Context of proposed survey.* A mid-infrared survey of the entire Galactic plane is complementary to existing and proposed surveys at shorter and longer wavelengths. A uniform, systematic survey at 3.6 and 4.5 $\mu$m will catalog protostars, evolved stars and highly obscured stars. Shorter wavelength observations (2MASS, UKIDSS) are not able to unambiguously detect and/or identify intrinsically red sources such as protostars and evolved stars. Figure 6, a color-color diagram from Whitney *et al.* [45], displays the location of main sequence stars, evolved stars and protostars on near and mid-IR color spaces. With just the addition of the 3.6 $\mu$m band, evolved stars are more clearly

separated from reddened early-type main sequence stars and protostars are distinguished from reddened late type giants. The 4.5 $\mu$m band provides even more leverage in color space (Gutermuth *et al.* [46]) distinguishing between class II and class III protostars.

Far-infrared and submillimeter observations are more sensitive to young protostars but current and future instruments are unable to match the resolution of IRAC. IRAC provides resolution $4\times$ that of Herschel's 70 $\mu$m band and $7\times$ that of the shortest passband of the JCMT Galactic plane survey. High resolution imaging is important for determining the multiplicity of star-forming regions (Allen *et al.* [47]). The multiplicity of star formation, particularly in massive star forming regions, is very sensitive to the formation mechanism and can be used to determine the relative roles of competitive accretion, turbulent fragmentation, etc.

*Implementation Plan.*   To complete the IRAC survey of the galactic disk, a program could be conducted during the Spitzer warm mission which would result in a 1250 square degree survey of the Galactic plane in two epochs. As the inner Galactic plane has already been observed by the GLIMPSE team, only one epoch for this region would be required. This survey would follow the warp and flare in the outer Galaxy as traced by molecular line surveys (Wouterloot *et al.* [48]). The survey region would include most of the molecular disk and the majority of star formation in the Galaxy. Figure 7 displays the proposed survey coverage in Galactic coordinates. The region of the plane within $|l| < 5°$ has been well mapped by Spitzer and does not require additional coverage.

The original GLIMPSE fields (light grey regions in Fig 7) require a single pass of one two second frame to improve radhit and solar-system object rejection. As the remainder of the survey region has a lower object density, we can integrate deeper before becoming confusion limited. With four 12 second integrations, the limiting magnitudes at 3.6 and 4.5 $\mu$m are 18.4 and 17.5, respectively. The sensitivity of the $|l| > 65°$ portion is well-matched to the ongoing UKIDSS survey and is considerably deeper ($10\times$) than the all-sky survey of WISE. The portion of the survey region in dark grey in Fig. 7 will be done with two epochs of two 12s high-dynamic range (HDR) integrations. HDR mode is necessary to recover the flux of bright sources (up to $\sim 1$ Jy). Four dithers are required for robust radhit rejection.

The GLIMPSE survey covered 220 square degrees in 400 hours with IRAC. The proposed observations would use a similar mapping strategy but would include an additional epoch and use 12 second HDR mode observations (which require 50% more time than the 2 second GLIMPSE observations). The estimated time for this very complete survey of the Galactic disk is $\sim 5500$ hours.

## 6.4.  Thermal Imaging of Extrasolar Giant Planet Transits

Despite exquisite ground-based and spacebourne measurements, current models of giant planets cannot even constrain the mass of the putative solid core at the center of Jupiter to a range smaller than 0 to 12 Earth masses. Yet core masses of giant planets are the most important parameter distinguishing the two currently competing theories of planet formation; core accretion (Mizuno [49], Hubickyj *et al.* [50]) and gravitational

**FIGURE 5.** Three color composite image of the young open cluster NGC 1893. 2MASS K$_s$ band data is displayed in blue, IRAC 3.6 $\mu$m is in green and IRAC 4.5 $\mu$m in red. Numerous protostars (red objects) are visible. The IRAC data is representative of the quality of the proposed survey.
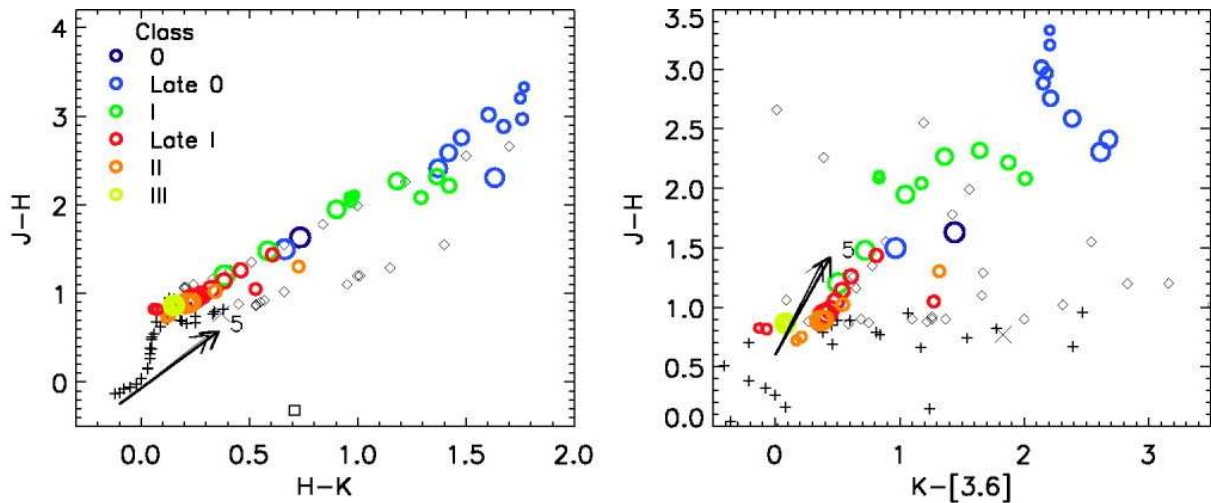


**FIGURE 6.** Near-IR and Near-IR with IRAC 3.6 $\mu$m color-color plots indicating the color space of main sequence stars (crosses), red giant and supergiant stars (diamonds), AGB stars (squares), planetary nebulae (asterisks), reflection nebulae (small crosses), T-tauri stars (large cross) and protostars (colored circles). Reprinted from Whitney *et al.* [45].
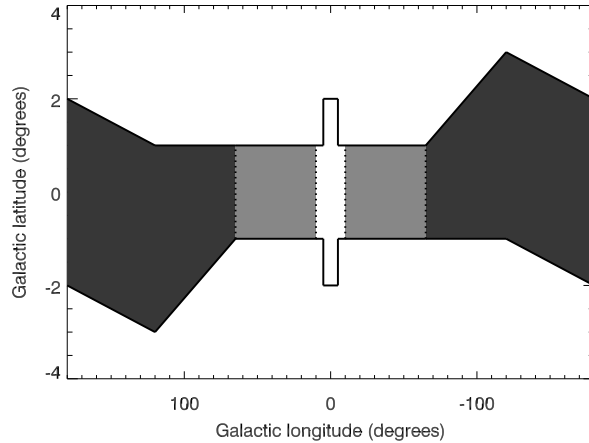
**FIGURE 7.** Coverage of the proposed Galactic plane survey. The field to be mapped with IRAC is outlined. The light gray regions need one additional epoch of 2 second integrations. The dark gray regions will be mapped by two epochs of two 12 second HDR exposures.

instability (Boss [51, 52]). The detection of the photometric signature of "hot Jupiters" transiting across the face of their parent stars has opened up a new and exciting means to study extrasolar giant planets (EGPs). By combining information from the radial velocity orbital solutions and the depth of the primary transit, it is possible to directly estimate the radii of the transiting EGPs. While the masses and radii determined for the 9 known EGPs are generally in accord with theoretical expectations, there are exceptions that continue to challenge our current understanding. By virtue of their size distribution, their extreme temperature ranges, and their growing number, transiting EGPs may be the most promising avenue of attacking the problem of planet formation.

For close-orbit, extrasolar giant planets (EGPs), the flux density contrast ratios between planet and star are approximately 2 orders of magnitude greater at 3 and 5 $\mu$m than they are at optical wavelengths. This relatively favorable flux contrast makes it possible to detect the secondary transit where the hot Jupiter is eclipsed by the parent star, if accurate mid-infrared photometry is available. IRAC has already demonstrated the required photometric stability by directly detecting the photons emitted by an EGP. Figure 8 shows the 4.5 $\mu$m time series photometry of the secondary eclipse of TrES-1 (Charbonneau *et al.* [53]), where the parent star is a K0 dwarf with V = 11.8. Together with similar 8 $\mu$m observations, these data have provided the first observational constraints on models of thermal emission and atmospheric constituents in hot Jupiters (Burrows [54]). There are now several Spitzer programs in progress to carry out photometry of transiting EGPs using IRAC, MIPS, and IRS.

By providing insights into the atmospheric constituents and thermal properties of EGPs, including heat transport from the day to night sides by winds and jet streams (which may measurably shift the light curves with respect to the orbital ephemeris), IRAC photometry can enable more stringent constraints to be placed on important model inputs, including bulk composition, the equation of state, and the degree of inhomogeneity (Guillot [55]). "Hot stratospheres", which are common to gas giants in
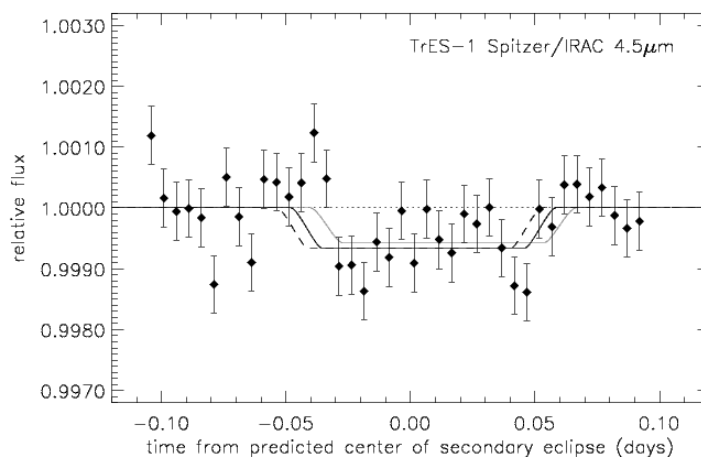
**FIGURE 8.** Binned IRAC 4.5 $\mu$m time series photometry of TrES-1. Reprinted from Charbonneau *et al.* [53].

our Solar System, and which have the effect of reducing planetary radii by absorbing heat high in the atmosphere rather than in the lower regions where stellar insolation can slow the normal contraction of the planet, will be most clearly seen in IRAC photometry (Fortney *et al.* [57]). Figure 9 compares measured IRAC fluxes for TrES-1 (Charbonneau *et al.* [53]) with model atmosphere predictions (Sudarsky *et al.* [60]) and clearly demonstrates weaknesses in the model. Agreement between theory and the observations can be significantly improved by increasing the metallicity of the model atmosphere by a factor of between 3 and 5 over solar (Fortney *et al.* [56]). 3.6 $\mu$m observations will enable much stronger constraints to be placed on the amount of atmospheric methane, and by extension on the efficiency of heat transport to the night side of the planet (Fortney *et al.* [57]).

For brighter systems such as HD 189733b (V = 7.7, sp. type K0V) and HD 209458 (V = 7.7, sp. type G0V), time series IRAC photometry will enable a search for longitudinal variations indicative of planetary weather. By gathering high-cadence photometric observations during secondary ingress and egress, it should be possible to detect differences in the shape of the light curve from the predictions of a uniformly illuminated disk. Model predictions (Williams [58]) have shown that the 3.6 and 4.5 $\mu$m channels should be particularly sensitive to realistic variations in the distribution of surface flux for systems like HD 209458b. Other models (Burrows *et al.* [59]) have shown that the relative flux in the 3.6 and 4.5 $\mu$m channels is sensitive to the details of the chemical composition in the stratosphere. Both the surface inhomogeneity detection and the chemistry model constraints will require high quality IRAC observations of many secondary eclipses per target.

Another application with a tremendous potential payoff is the measurement of temperature gradients across the surfaces of hot EGPs. Understanding how the intense stellar insolation is absorbed and reradiated is fundamental to an understanding of their atmospheric physics. Using time series, 24 micron MIPS photometry, Harrington *et al.* [61]
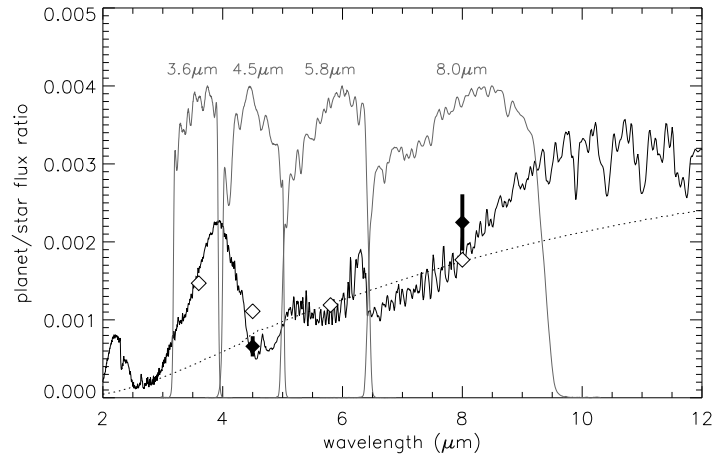
**FIGURE 9.** Predicted planet/star flux ratios from a model hot jupiter spectrum (Sudarsky *et al.* [60]), compared with IRAC measurements (Charbonneau *et al.* [53]) for TrES-1 (filled diamonds). The dotted line shows a blackbody spectrum corresponding to a temperature of 1060 K. The open diamonds show the expected flux in each IRAC waveband. Note the substantial overprediction of flux at 4.5 $\mu$m , suggesting a significant additional source of atmospheric opacity near 4$\mu$m. Reprinted from Charbonneau *et al.* [53].

recently demonstrated the existence of a large asymmetry in the temperatures of the day and night sides of $\upsilon$ Andromeda b. The conclusion they draw is that most of the incident stellar radiation is reemitted at the subsolar point, with very little heat transport to the night side of the planet. The technique relies solely on the brightness modulation of the planet as it orbits its parent star and does not require a transiting geometry. The method is thus potentially applicable to all known hot EGPs. While the planet/star flux ratio is more favorable at 24 microns for EGPs in the $\sim 1000 - 2000$ K range, this ratio is no more than 1.7 to 5 times smaller at 4.5 microns (depending on relative temperatures of star and planet), with typical values of around $\sim 2.5$. There are currently 53 EGPs known with semi-major axes of less than 0.1 AU (that of $\upsilon$ Andromeda is 0.06 AU). With a sufficient investment of observing time, IRAC should therefore enable us to better characterize the atmospheres of a significant number of hot, non-transiting EGPs.

How many transiting EGPs will be available during Spitzer's warm mission? The COROT mission (scheduled for launch in December, 2006) is expected to yield on the order of 45 transiting EGPs with $11 < m_v < 16.5$ over the course of its 2.5 year mission (Gillon *et al.* [62]). The first public data release is currently expected to occur during the summer of 2008, with subsequent data releases every 6 to 12 months. The time frame is thus well matched to post-cryogen, IRAC followup observations.

The launch date for Kepler currently remains November, 2008. Whereas the detection of terrestrial-mass planets is expected to require most of the 4 year mission, hot Jupiters will be readily detectable within the first year. The Kepler project has offered to communicate such detections in advance of publication (Borucki, 2007, private comm.). The time frame for the first such detections would therefore be late 2009, near the time when Spitzer exhausts its cryogen supply. Though estimates are necessarily model dependent,

the expectation is that Kepler will detect on the order of 100 giant inner planets in the first year for stars with $9 < m_v < 14$ (for comparison, the parent star for TrES-1 has $m_v = 11.8$). The discovery of an additional $\sim 30$ outer-orbit giant planets is expected over the life of the mission.

In addition to Kepler and COROT, there are at least a dozen ground-based, photometric transit surveys active at the present time (Charbonneau *et al.* [63]). With a sustained and distributed effort of this magnitude, it is reasonable to expect that the number of known transiting giant planets will increase substantially over the next several years, even without the Kepler detections. Roughly half of these transit surveys utilize a small-aperture, wide-field approach, and are primarily sensitive to relatively bright parent stars (V < 10). These stars will be particularly good targets for precision photometry with the IRAC 3.6 and 4.5 $\mu$m channels, which will be the most sensitive available probes of EGP atmospheres until the launch of JWST.

Each monitoring observation of an EGP (one filter, one eclipse) takes of order 8 hours to cover the ingress, eclipse and egress and to define well the out-of-eclipse continuum level. If for a given IRAC channel five secondary-transits are monitored (to improve the S/N over a single measurement), and if data are obtained in both IRAC channels, the average exposure time per target would be of order 80 hours. Obtaining complete secondary transit data for 20 target stars would therefore require of order 1500 hours of Spitzer observing time. We note that at the current rate of detection of transiting planets by ground-based campaigns, we would expect more than enough targets to be available even without data from COROT or Kepler.

# ACKNOWLEDGMENTS

# REFERENCES

1. Fazio, G., *et al.*, 2004, ApJS, 154, 10
2. McMurtry, C., Pipher, J., and Forrest, W., 2006, SPIE, 6265E, 6
3. Lonsdale, C. J., *et al.*, 2003, PASP, 115, 897
4. Lonsdale, C., *et al.*, 2004, ApJS, 154, 54
5. Oliver, S., *et al.*, 2004, ApJS, 154, 30
6. Babbedge, T. S. R., *et al.*, 2006, MNRAS, 676
7. Rowan-Robinson, M., *et al.*, 2005, AJ, 129, 1183
8. Farrah, D., *et al.*, 2006, ApJL, 641, L17
9. Ilbert, O. 2006, A&A, 457, 841
10. Sawicki, M. 2002, AJ, 124, 3050
11. Gladders, M. D., and Yee, H. K. C. 2000, AJ, 120, 2148

12. Refregier, A. 2003, ARA&A, 41, 645
13. Schneider, P. in *Gravitational Lensing : Strong, Weak & Micro. Saas-Fee Advanced Course 33*, edited by G. Meylan, P. Jetzer and P. North, Springer-Verlag, Berlin, 2006, 273 (astro-ph/0509252)
14. Hoekstra, H. 2006, ApJ, 647, 116
15. Labbé, I., *et al.*, 2005, ApJL, 624, L81
16. Shapley, A. E., *et al.*, 2005, ApJ, 626, 698
17. Rigopoulou, D. 2006, ApJ, 648, 81
18. Croton, D. J., *et al.*, 2006, MNRAS, 365, 11
19. Cutri, R. M., Nelson, B. O., Francis, P. J., and Smith, P. S., in *AGN Surveys*, IAU Colloq. 184, edited by R. F. Green, E. Y. Khachikian, and D. B. Sanders, ASP Conference Series 284, ASP, San Francisco, 2002, 127
20. Glikman, E., Gregg, M. D., Lacy, M., Helfand, D. J., Becker, R. H., and White, R. L. 2004, ApJ, 607, 60
21. Warren, S. J., Hewett, P. C., and Foltz, C. B. 2000, MNRAS, 312, 827
22. Sanders, D. B., Soifer, B. T., Scoville, N. Z., and Sargent, A. I. 1988, ApJL, 324, L55
23. Lawrence, A. 1991, MNRAS, 252, 586
24. Dickinson, M. Giavalisco, M., and The GOODS Team, "The Great Observatories Origins Deep Survey" in *The Mass of Galaxies at Low and High Redshift*, edited by R. Bender and A. Renzini, Springer-Verlag, Berlin, 2003, pp. 324-331.
25. Chary, R. *et al.*, 2007, ApJ, submitted
26. Yan, H., Dickinson, M., Giavalisco, M., Stern, D., Eisenhardt, P. R. M., Ferguson, H. C., ApJ, 651, 24
27. Eyles, L., Bunker, A., Stanway, E., Lacy, M., Ellis, R., and Doherty, M. 2005, MNRAS, 364, 443
28. Springel, V. *et al.*, 2005, Nature, 435, 629
29. Wilkinson, M. *et al.*, 2006, EAS, 20, 105
30. Bouwens, R. J. *et al.*, 2006, ApJ, 653, 53
31. Heger, A., *et al.*, 2003, ApJ, 591, 288
32. Scannapieco, E., *et al.*, 2005, ApJ, 633, 1031
33. Kashlinsky, A., *et al.*, 2005, Nature, 438, 45
34. Benjamin, R. A. *et al.*, 2003, PASP, 115, 953
35. Stolovy, S., *et al.*, 2006, J. Physics, Conf. Vol 54, pp. 176-182
36. Mercer, E. P., *et al.*, 2005, ApJ, 635, 560
37. Mercer, E. P., *et al.*, 2004, ApJS, 154, 328
38. Benjamin, R. A. *et al.*, 2005, ApJL, 630, 149
39. Kobayashi, N., Yasui, C., Tokunaga, A., Saito, M., 2005, Protostars and Planets V LPI Contribution 1286, 8639, http://www.lpi.usra.edu/meetings/ppv2005/pdf/8639.pdf
40. Shara, M. M., Moffat, A. F. J., Smith, L. F., Niemela, V. S., Potter, M., and Lamontagne, R. 1999, AJ, 118, 390
41. Caber-Lavers, A., Garzón, and Hammersley, P. L. 2005, A&A, 433, 173
42. Marshall, D. J., Robin, A. C., Reylé, C., Schultheis, M., and Picaud, S. 2006, A&A, 453, 635
43. Frieswijk, W. F. W., Teyssier, D., Shipman, R. F., Hily-Blant, P., 2005, Protostars and Planets V LPI Contribution 1286, 8582, http://www.lpi.usra.edu/meetings/ppv2005/pdf/8582.pdf
44. Weingartner, J. C., and Draine, B. T. 2001, ApJ, 548, 296
45. Whitney, B. A., Wood, K., Bjorkman, J. E., and Cohen, M. 2003, ApJ, 598, 1079
46. Gutermuth, R. A., Megeath, S., Muzerolle, J., Allen, L., Pipher, J., Myers, P., and Fazio, G., 2004, ApJ, 154, 374
47. Allen, L. E., *et al.*, 2005, in *Protostars and Planets V*, edited by B. Reipurth, D. Jewitt and K. Keil, Univ. Arizona Press, Tucson, 2007, pp. 361-376
48. Woulterloot, J. G. A., Brand, J., Burton, W. B., and Kwee, K. K. 1990, A&A, 230, 21
49. Mizuno, H. 1980, Prog. Theor. Phys., 64, 544
50. Hubickyhj, O., Bodenheimer, P., and Lissauer, J. 2004, in *Gravitational Collapse: From Massive Stars to Planets* edited by G. Garcia-Segura et al., Rev. Mex. AA Ser. Conf., pp. 83-86
51. Boss, A. P. 1997, Science, 276, 1836
52. Boss, A. P. 2004, ApJ, 610, 456
53. Charbonneau, D., *et al.*, 2005, ApJ, 626, 523
54. Burrows, A. 2005, Nature, 433, 261

55.  Guillot, T. 2005, Ann. Rev. of Earth and Plan. Sci., 33, 493
56.  Fortney, J. J., Marley, M. S., Lodders, K., Saumon, D., and Freedman, R. S. 2005, ApJ, 627, L69
57.  Fortney, J. J., Saumon, D., Marley, M. S., Lodders, K., and Freedman, R. S. 2006, ApJ, 642, 495
58.  Williams, P. K. G., Charbonneau, D., Copper, C. S., Showman, A. P., and Fortney, J. J. 2006, ApJ, 649, 1020
59.  Burrows, A., Sudarsky, D., and Hubeny, I. 2006, ApJ, 650, 1140
60.  Sudarsky, D., Burrows, A., and Hubeny, I. 2003, ApJ, 588, 1121
61.  Harrington, J., *et al.*, 2006, Science, 314, 623
62.  Gillon, M., Courbin, F., Magain, P., and Borguet, B. 2005, A&A, 442, 731
63.  Charbonneau, D., Brown, T. M., Burrows, A., and Laughlin, G., in *Protostars and Planets V*, edited by B. Reipurth, D. Jewitt and K. Keil, Univ. Arizona Press, Tucson, 2007, pp. 701-716